Publ. Nr. 96/13

CHALMERS TEKNISKA HÖGSKOLA
Institutionen för Termo- och Fluiddynamik

CHALMER UNIVERSITY OF TECHNOLOGY
Department of Thermo- and Fluid Dynamics

The Two-Equation Turbulence k-ω Model Applied to Recirculating Ventilation Flows

by

Shia-Hui Peng, Lars Davidson, Sture Holmberg

Göteborg, February 1996

The Two-Equation Turbulence k-ω Model Applied to Recirculating Ventilation Flows{ }

Shia-Hui Peng[1, 2], Lars Davidson[1], Sture Holmberg[2]
1 Thermo and Fluid Dynamics, Chalmers University of Technology, S-412 96 Gothenburg, Sweden
2 Ventilation Technology, National Institute for Working Life, S-171 84 Solna, Sweden

Abstract *An investigation of the performance of the two-equation turbulent k-ω model has been conducted for recirculating flows in ventilated spaces. In conjunction with either the wall-function method or an extended-to-wall method, the original k-ω model of Wilcox was compared with the standard and low-Reynolds-number k-ε models. It was found that the original k-ω model predicts a longer reattachment length for the flow over a backward-facing step with a large expansion ratio to which the mixing room ventilation is relevant. In order to enhance the accuracy in predicting ventilation flows, some modifications to the original k-ω model were proposed. A turbulent cross-diffusion term was added to the ω-equation in analogy to its molecular counterpart. Several model coefficients were re-evaluated in an attempt to find the optimum choice. The behavior of both the original and modified k-ω models was analyzed, and the computational efforts with different models to achieve a converged solution were compared. The modified model is shown to be more robust in convergence.*

In comparison with both experimental data and predictions by other models, the results calculated by the modified model are quite encouraging. It is shown that this model can be an alternative to the conventional k-ε model for calculating complex ventilation flows. With the extended-to-wall method, the k-ω model integrates the solution directly to the wall surface without using any damping functions, and the prediction accuracy for mean flow profiles is generally similar to that with the Lam-Bremhorst low-Reynolds-number (LRN) k-ε model. Without suffering the uncertainty from specifying ε at the wall surface, the k-ω model uses an exact asymptotic solution as the boundary condition of ω when using the extended-to-wall method. The solution procedure usually is more stable than using an LRN k-ε model.

Nomenclature

c_μ, c_ω	model constants
E	constant in Eq. (29)
h	height of inlet
H	height of computational domain
k	turbulent kinetic energy
I_{in}	turbulence intensity at inlet
k_{in}	turbulent kinetic energy at inlet
l_{in}	turbulent length scale at inlet
p	pressure
Re	inlet-based Reynolds number
T	height of outlet
U_0, u_{in}	velocity at inlet
u_i	velocity components in Cartesian coordinates
u_τ	friction velocity
u', v'	fluctuating velocities in x- and y-directions respectively
W	height of backward-facing step
x_i	coordinate directions (x, y)
x_r	reattachment length
y^+	dimensionless distance from wall surface, $u_\tau y/\nu$

Greek letters

α, α^*	model constants
β, β^*	model constants
δ_{ij}	Kroneker delta
ε	dissipation rate of k
ε_{in}	dissipation rate of k at inlet
κ	von Kármán constant
γ	coefficient in Eq. (20)
μ	molecular viscosity
μ_t	turbulent eddy viscosity
ν	kinematic molecular viscosity
ν_t	kinematic turbulent viscosity
ρ	density of air
σ_k, σ_ω	model constants
τ	turbulence time scale
ω	specific dissipation rate of k
ω_{in}	specific dissipation rate of k at inlet

1 Introduction

Recirculating flow phenomena exist in most ventilated spaces where an efficient mixture with supplied fresh air is required to dilute the contaminants. With a mixing ventilation system, for example, fresh air is ejected into the room through an inlet under the ceiling to produce an overall recirculation which greatly affects the indoor air quality, thermal comfort and energy consumption. Recirculation is also a powerful generator of turbulence and hence mixing and losses. This flow phenomenon, therefore, has been the subject of many studies, particularly for benchmarking the performance of turbulence models, e.g. in [1] and [2].

The standard high-Reynolds-number k-ε model is reasonably well-behaved in conjunction with either wall functions or low-Reynolds-number corrections, and has been widely used for solving a variety of ventilation problems. Nevertheless, the k-ε model has some limitations when used for simulating indoor air flows and heat transfer, as documented by Chen and Jiang [3]. In addition, local laminar regions usually exist in a ventilated space, not only in the near-wall region but also in areas far from the wall surface. For example, in the flow field created with a displacement ventilation system where the fresh air is supplied at a small velocity and with a lower temperature than the ambient air, an upwards plume-like air flow with some laminar characteristics is triggered in the lower zone of the ventilated space owing to the influence of buoyancy. Davidson [4] showed that a low-Reynolds-number k-ε model usually renders this flow a *pure* and practically untrue laminar solution. The k-ω model, by contrast, is expected to be able to reasonably capture the characteristics of this type of flow because the ω-equation possesses a solution as the turbulent kinetic energy approaches zero. To accurately simulate complex ventilation flows, investigating the performance of various turbulence models therefore becomes increasingly important.

Over the past two decades, several alternative two-equation turbulence models have been developed, including the k-kl model by Rotta [5], the k-$k\tau$ model by Zeierman and Wolfshtein [6] and the k-τ model by Speziale et al [7]. Most notably, a significant development has been made on the two-equation k-ω model and/or its variants [8]-[12]. A standard k-ω model, which is well-developed for engineering applications, has been proposed by Wilcox [11]. This model is capable of yielding more accurate results than other two-equation models for predicting adverse pressure gradient flows and separate flows, as reported by Wilcox [11] and Menter [13]. Liu and Zheng [14] applied this model to solving cascade flows, and obtained predictions in good agreement with experimental data. Patel and Yoon [15] used it for separated flows over rough surfaces, and the results were shown to be remarkably accurate compared to those by k-ε models. More recently, a low-Reynolds-number k-ω model has been proposed by Wilcox [12] for simulating transitional incompressible flat-plate boundary layer flows, realistic descriptions on the transitional regions were reported. The advantages of the k-ω model have emerged mainly in aerodynamic applications. For predicting recirculating ventilation flows, however, the performance of this model remains unclear.

Unlike with the standard k-ε model, the solution of Wilcox's standard k-ω model can be integrated directly to near-wall regions without using the wall functions as a bridge, i.e. with the *extended-to-wall* method. In contrast to the uncertain determination of ε on a wall surface when using LRN k-ε models, the wall boundary condition of ω is replaced with its exact asymptotic solution in the immediate wall proximity. With the extended-to-wall method, a refined grid must be employed to resolve near-wall behaviors of turbulence. To avoid a high computer power requirement, on the other hand, the standard k-ω model can also be used in conjunction with the wall-function method in engineering applications.

This paper implements the *k*-ω model to simulate recirculating ventilation flows, and investigates the model's performance. It was found that Wilcox's original *k*-ω model overpredicts the reattachment length for a backward-facing step flow with a large expansion ratio. Modifications to this model are proposed to enhance its prediction accuracy. The physical arguments with the modification are described. A turbulent cross-diffusion term is added to the ω-transport equation, and the closure constants are re-evaluated by a straightforward argument within the context of two-equation turbulence models. In conjunction with either the wall-function method or the extended-to-wall method, calculations were performed for two typical flows relevant to room ventilation, including a separated flow over a backward-facing step with a large expansion ratio and a recirculating flow in a two-dimensional confined enclosure. Comparisons were made between predictions and experiments, and between predictions with various two-equation turbulence models. The behavior of the *k*-ω model was analyzed. The computational effort to achieve a converged solution with various models was discussed based on the calculation of the recirculating flow in the confined enclosure.

2 Model Formulation

This section describes the mathematical formulation of the *k*-ω model, including the governing equations, the physical arguments for the modification, and the boundary conditions.

2.1 Governing Equations

By using Boussinesq's hypothesis, the governing equations of Wilcox's original *k*-ω model [11] for steady-state turbulent flow are as follows.

For continuity,

$$\frac{\partial(\rho u_i)}{\partial x_i} = 0 \tag{1}$$

For momentum,

$$\frac{\partial(\rho u_j u_i)}{\partial x_j} = -\frac{\partial p}{\partial x_i} + \frac{\partial}{\partial x_j}\left[(\mu + \mu_t)\frac{\partial u_i}{\partial x_j}\right] \tag{2}$$

For turbulent kinetic energy *k*,

$$\frac{\partial(\rho u_j k)}{\partial x_j} = P_k - \beta^* \rho\omega k + \frac{\partial}{\partial x_j}\left[\left(\mu + \frac{\mu_t}{\sigma_k}\right)\frac{\partial k}{\partial x_j}\right] \tag{3}$$

For specific dissipation rate of *k*,

$$\frac{\partial(\rho u_j \omega)}{\partial x_j} = \alpha\frac{\omega}{k}P_k - \beta\rho\omega^2 + \frac{\partial}{\partial x_j}\left[\left(\mu + \frac{\mu_t}{\sigma_\omega}\right)\frac{\partial \omega}{\partial x_j}\right] \tag{4}$$

The production of kinetic energy, P_k , for incompressible flows is expressed by

$$P_k = \mu_t \left(\frac{\partial u_i}{\partial x_j} + \frac{\partial u_j}{\partial x_i} \right) \frac{\partial u_i}{\partial x_j} \tag{5}$$

The eddy viscosity, μ_t, is defined in terms of the turbulent kinetic energy k and the specific dissipation rate ω:

$$\mu_t = \alpha^* \frac{\rho k}{\omega} \tag{6}$$

In Wilcox's model, the closure constants are determined as $\alpha^* = 1.0$, $\beta^* = 0.09$, $\alpha = 0.56$, $\beta = 0.075$ and $\sigma_k = \sigma_\omega = 2.0$.

2.2 Arguments for Model Modification

The Turbulent Cross-Diffusion Term. In the above equations, the k-equation is directly modelled after the time-averaged, exact equation for the turbulent kinetic energy. This equation is thus consistent with the one in other two-equation models. As Wilcox indicated, however, the greatest amount of uncertainty and controversy usually lies in the scale-determining equation, i.e. the ω-equation. Indeed, the calculations for channel flows [17] pointed out that the original model returns a too-low near-wall peak of the turbulent kinetic energy owing to the specific dissipation rate overpredicted. This in turn makes the near-wall eddy viscosity underestimated.

The relation between ω and ε can be written as

$$\omega = \frac{\alpha^* \varepsilon}{c_\mu k} \tag{7}$$

where $c_\mu = 0.09$, a model constant in the standard k-ε model. Equation (7) implies that the specific dissipation rate ω is equivalent to the rate of dissipation of turbulence per unit kinetic energy. On the other hand, ω can also be regarded as a reciprocal of turbulent time scale or the so-called *turnover time* of turbulence $\tau = k/\varepsilon$. Since $D\omega/Dt = (D\varepsilon/Dt)/k - \omega(Dk/Dt)/k$, the exact ω-transport equation can be derived with the aid of the exact ε-equation and k-equation, and takes the form:

$$\frac{\partial(\rho u_j \omega)}{\partial x_j} = \left(\frac{P_\varepsilon}{k} - \frac{\omega P}{k} \right) + \left(\rho \omega^2 - \frac{\Pi_\varepsilon}{k} \right) + \left(\frac{\omega D}{k} - \frac{D_\varepsilon}{k} \right) + \left(\mu \frac{\partial^2 \omega}{\partial x_j \partial x_j} + \frac{2\mu}{k} \frac{\partial \omega}{\partial x_j} \frac{\partial k}{\partial x_j} \right) \tag{8}$$

where P_ε, Π_ε and D_ε are the production, destruction and diffusive transport terms respectively in the exact ε-equation, while P and D are the production term and transport term in the exact k-equation. As with other turbulence transport equations, the convection of the specific dissipation rate ω is balanced by its production, destruction, and turbulent and molecular diffusion on the right-hand side of equation (8).

Inspecting the exact ω-equation suggests that it is more reasonable to model the turbulent diffusion term in analogy to its viscous counterpart, i.e.

$$D_\omega = \left(\frac{\omega D}{k} - \frac{D_\varepsilon}{k} \right) = \left[\frac{\partial}{\partial x_j} \left(\frac{\mu_t}{\sigma_\omega} \frac{\partial \omega}{\partial x_j} \right) + c_\omega \frac{\mu_t}{k} \left(\frac{\partial k}{\partial x_j} \frac{\partial \omega}{\partial x_j} \right) \right] \tag{9}$$

Wilcox [11] neglected the viscous cross-diffusion term and modelled the turbulent diffusion without employing the turbulent cross-diffusion term, see equation (4). It can be argued that it is the exclusion of the viscous cross-diffusion term that leads to the incorrect asymptotic behavior of the turbulent kinetic energy [7]. However, if the viscous cross-diffusion term remains in the *modelled* ω-equation as the wall approaches, i.e.

$$\mu\frac{\partial^2\omega}{\partial^2 y}+\frac{2\mu}{k}\frac{\partial\omega}{\partial y}\frac{\partial k}{\partial y}-\beta\rho\omega^2=0 \tag{10}$$

then the asymptotic analysis to equation (10) indicates that a negative specific dissipation rate will result unless the modelled destruction term is positive, which contradicts the realizability principle of turbulence modelling by Lumley [18]. In addition, the influence of the viscous cross-diffusion term is negligible in areas where the turbulence is fully developed and $\mu << \mu_t$. The viscous cross-diffusion term is thus omitted in the present modified ω-equation.

On the one hand, the addition of the turbulent cross-diffusion term in the ω-equation has no effect on the near-wall asymptotic behavior of both k and ω. On the other hand, this term may play a non-negligible role in transporting the turbulent kinetic energy and its specific dissipation rate in turbulent recirculating flows. Near the wall, the gradients of k and ω are of opposite sign, the term as a whole reduces ω and hence raises k as desired. With the new turbulent cross-diffusion term included, the modified ω-equation becomes

$$\frac{\partial(\rho u_j\omega)}{\partial x_j}=\alpha\frac{\omega}{k}P_k-\beta\rho\omega^2+\frac{\partial}{\partial x_j}\left[\left(\mu+\frac{\mu_t}{\sigma_\omega}\right)\frac{\partial\omega}{\partial x_j}\right]+c_\omega\frac{\mu_t}{k}\left(\frac{\partial k}{\partial x_j}\frac{\partial\omega}{\partial x_j}\right) \tag{11}$$

The Values of the Constants. Wilcox's original k-ω model was applied to the backward-facing step flow with a large expansion ratio (W/h = 5), which is relevant to the general situation of room ventilation with a mixing system where the air-supply inlet is usually installed under ceiling. It was found that the predicted reattachment length was longer than the measured by Restivo [16]. This inaccuracy agrees with the fact found in the calculations for channel flows [17] where the near-wall turbulent kinetic energy is underpredicted by the turbulence equations in the original model. The straightforward remedy is to suppress the specific dissipation rate by reducing its production through constant α in the ω-equation, i.e. equation (11). Consequently the turbulent kinetic energy can be enhanced. To refine the closure constants, several conditions must be taken into account in order not to break the physical argument for modelling two-equation turbulence models.

In the wall-layer of a local-equilibrium boundary layer flow, the log-law is valid. Using this relation and assuming that the production equals the dissipation of turbulent kinetic energy, one gets

$$\sqrt{\alpha^*\beta^*}=\frac{u_\tau^2}{k}=\frac{-\overline{u'v'}}{k} \tag{12}$$

Experimental data indicate that $u_\tau^2/k \approx 0.3$, which gives

$$\alpha^*\beta^*=0.09 \tag{13}$$

This is one of the important pre-conditions to correctly predict the constant-stress layer.

Under the condition of a decaying homogeneous, isotropic turbulence, equations (4) and (11) become

$$\frac{dk}{dx} = -\beta^* \omega k, \quad \frac{d\omega}{dx} = -\beta \omega^2 \tag{14}$$

This gives the solution to k as

$$k = x^{-\beta^*/\beta} \tag{15}$$

Experiments suggest that the exponent (β^*/β) has a value of 1 ~ 1.25 during the initial period of the decaying turbulence. Equation (15) thus requires that

$$\beta^* / \beta = 1 \sim 1.25 \tag{16}$$

Furthermore, an additional constraint is imposed in the reduced ω-equation when the logarithmic velocity distribution is applied to zero-pressure-gradient local-equilibrium boundary layer flows. This gives

$$\alpha = \beta / \beta^* - \frac{\kappa^2}{\sigma_\omega \sqrt{\alpha^* \beta^*}} \tag{17}$$

Equations (13), (16) and (17) form the prerequisites for refining the closure constants of the standard k-ω model. The re-established model constants, therefore, must satisfy with these conditions.

As indicated by Wilcox [11], setting $\alpha^* = 1$ possesses the generality of using other values for α^*. Indeed, it can be theoretically shown that varying α^* only alters the ω-distribution by a factor of α^*; the kinetic energy and thus the eddy viscosity will remain unchanged if equation (13) holds. Model constants σ_k and σ_ω, which control the diffusion rate of turbulence from higher-level regions to lower-level ones, are usually obtained by computer optimization. The inclusion of the turbulent cross-diffusion term may reinforce the transport of ω. To render a compatible transport for k, the diffusion of the turbulence energy thus needs to be enhanced. This can easily be achieved by setting $\sigma_k < \sigma_\omega$. The coefficient of the turbulent cross-diffusion term, c_ω, can be reproduced from the standard k-ε model by transforming the ε-equation into an ω-equation, which gives $c_\omega \sim (2.0/\sigma_\varepsilon)$, where σ_ε is the coefficient for the diffusion term in the ε-equation. Nevertheless, c_ω was also optimized in this study. The results calculated by the modified k-ω model were found to be fairly insensitive to the constant c_ω in the range between 0.6 and 1.25.

Based on the above arguments, the closure constants for the modified k-ω model have been established as follows

$$\alpha^* = 1.0,\ \alpha = 0.42,\ \beta^* = 0.09,\ \beta = 0.075,\ c_\omega = 0.75,\ \sigma_k = 0.8,\ \sigma_\omega = 1.35 \tag{18}$$

2.3 Boundary Conditions

Inlet. The k-ω model takes ω instead of ε as an independent variable. The velocities across the inlet boundary are usually prescribed. The turbulent kinetic energy and its specific dissipation

rate are specified either by the pre-calculated distributions in the channel flow or by the following equations

$$k_{in} = 1.5(I_{in} u_{in})^2, \quad \varepsilon_{in} = c_D k_{in}^{3/2} / l_{in} \tag{19}$$

$$\omega_{in} = \frac{c_\mu \varepsilon_{in}}{\alpha^* k_{in}} = \gamma \frac{\sqrt{k_{in}}}{l_{in}} \tag{20}$$

Here, the turbulence length scale at the inlet, l_{in}, is usually set as a fraction of the whole inlet height, and c_D is a constant. In the present calculations, the Lam-Bremhorst LRN k-ε model was used to get the distributions of the variables in channel flows, which then were used as the inlet profiles for calculating the backward-facing step flow. When computing the flow in the two-dimensional confined enclosure, the inlet conditions were specified by equations (19) and (20).

Outlet. The streamwise derivatives of the flow variables were set to zero at the outlet for calculating the backward-facing step flow, i.e.

$$\frac{\partial \phi}{\partial n} = 0 \qquad (\phi = u,\ v,\ k,\ \omega \ldots\ldots) \tag{21}$$

Moreover, it is necessary to ensure global mass conservation. When calculating the flow in the confined enclosure, the velocity was required to satisfy the following relation along the boundaries of the computational domain

$$\int_c \rho \mathbf{u} \cdot \mathbf{n}\, ds = 0 \tag{22}$$

where c is the boundary of the computational domain with $\mathbf{n}$ as the normal direction, and the other variables are specified according to equation (21).

Wall Boundary. The ω-equation has an exact solution in the immediate proximity of a wall surface where the viscous diffusion balances the destruction. With a refined grid in near-wall regions, this asymptotic solution is used to calculate the specific dissipation rate ω at the first node close to the wall surface. In the present calculations, at least one node is required below $y^+ = 5$. This makes it possible to integrate the solution of the k-ω model directly into the viscous sublayer without using the conventional wall functions or low-Reynolds-number corrections as a bridge. In such an extended-to-wall method, a zero value can be imposed at the wall for the velocity components and the turbulent kinetic energy, i.e.

$$u = v = 0, \quad k = 0 \tag{23}$$

The exact limit for ω is

$$\omega \to \frac{6\nu}{\beta y^2} \text{ as } y \to 0 \tag{24}$$

When using the Lam-Bremhorst LRN k-ε model, the boundary value of ε at the nodes closest to the wall surface is specified as

$$\varepsilon = \nu \frac{\partial^2 k}{\partial^2 n} \tag{25}$$

In engineering applications the wall-function method is often preferred to avoid a highly refined grid near the wall. The wall functions used with the *k*-ω model can be derived by simplifying the model equations in the logarithmic layer of a boundary layer flow as

$$\frac{\partial}{\partial y}\left(\nu_t \frac{\partial u}{\partial y}\right) = 0 \tag{26}$$

$$\nu_t \left(\frac{\partial u}{\partial y}\right)^2 - \beta^* \omega k + \frac{\partial}{\partial y}\left[\left(\frac{\nu_t}{\sigma_k}\right)\frac{\partial k}{\partial y}\right] = 0 \tag{27}$$

$$\alpha \alpha^* \left(\frac{\partial u}{\partial y}\right)^2 - \beta \omega^2 + \frac{\partial}{\partial y}\left[\left(\frac{\nu_t}{\sigma_\omega}\right)\frac{\partial \omega}{\partial y}\right] + c_\omega \frac{\nu_t}{k}\left(\frac{\partial k}{\partial y}\frac{\partial \omega}{\partial y}\right) = 0 \tag{28}$$

The velocity profile is assumed to obey the logarithmic law. It can be shown that the following is satisfied with equations (26)-(28) along a smooth wall surface

$$u = \frac{u_\tau}{\kappa}\ln(E y^+),\ k = \frac{{u_\tau}^2}{\sqrt{\alpha^* \beta^*}},\ \omega = \sqrt{\frac{\alpha^*}{\beta^*}}\frac{u_\tau}{\kappa y} \tag{29}$$

Equation (29) serves as the wall functions for both the modified and the original *k*-ω models in the calculations.

3 Numerical Method

The differential equations for *k* and ω, together with those governing the velocity components, were solved with a computer code CALC-BFC [19]. A collocated grid was used, in which all variables are stored at the center of the same control volume. To avoid the unphysical oscillations in the pressure field owing to using a collocated grid, see Patankar [20], the Rhie-Chow interpolation method [21] was used to calculate the velocity components at the control volume faces.

In order to reduce numerical diffusion, the convection terms in the momentum equations were discretized by the third-order accurate QUICK scheme of Leonard [22], which is an upwind-biased scheme and is hence stable for solving recirculating flows of elliptic nature. The hybrid scheme [20] was applied to the convection terms in the *k* and ω equations, and the central differencing scheme was used to deal with the diffusion terms. In the discrete ω-equation, the turbulent cross-diffusion term was added to the right-hand-side of the algebraic equation when it was positive, otherwise to the left-hand-side.

The discrete algebraic equations were solved with an iterative procedure, and the under-relaxation method was used to promote the solution stability. The SIMPLEC algorithm was used to deal with the coupling between the pressure and the velocity. The solution of algebraic equations for the velocity components was achieved by applying the Tri-Diagonal Matrix Algorithm (TDMA), and the pressure correction equation was solved with the Strongly Implicit Procedure (SIP) algorithm [23].

A solution procedure was terminated when the normalized sum of absolute cell residuals satisfies

$$\frac{\sum |R^k|}{F_n} \le \lambda \tag{30}$$

In equation (30), F_n is typically the inlet momentum flux, R is the residual of the algebraic equations, and λ is a convergence criterion, which was of the order of 10^{-3}.

The solution is usually affected by the grid arrangement. In particular, when the calculation is used to verify the turbulence models, the grid-independent solution is desired. The way to determine the number of the grid nodes is to perform calculations with gradually refined grids until no obvious difference occurs between the solutions with two grids. This practice was adopted here.

4 Results and Discussion

The calculation for the backward-facing step flow is first carried out. The recirculating flow in a two-dimensional confined enclosure is then considered. Results between various models and experimental data are compared. The model behavior is analyzed and the effect of the modification is discussed.

4.1 Backward-Facing Step Flow

The flow over a backward-facing step with a large expansion ratio is relevant to room ventilation with a mixing system where fresh air is often supplied through a slot under ceiling to create recirculation and mixing. The air velocity at the inlet should be large enough to fully dilute the indoor contaminants with the induced flow field. On the other hand, this velocity is limited to avoid the potential local drafts, which are associated with the local air velocity and turbulence level in the flow domain. The backward-facing step geometry used here has an expansion ratio of W:h = 5:1, see Figure 1.

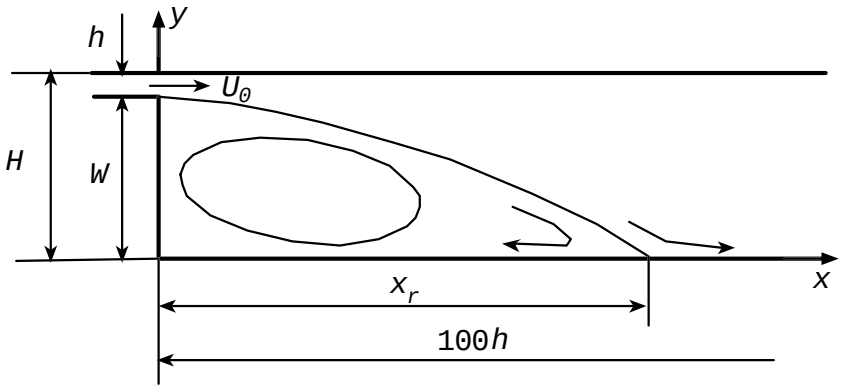

Figure 1. Backward-facing step configuration.

The distributions of the velocity, turbulent kinetic energy and its dissipation rate at the inlet were specified by solving for channel flows with the Lam-Bremhorst LRN k-ε model [24]. The inlet ω-profile was obtained from equation (7), which ensures an identical distribution of the eddy viscosity at the inlet whether using the k-ω model or the standard k-ε model (SKE). With the k-ω model, two methods were applied as described in Section 2, i.e. the *extended-to-wall*

method (Eqs. (23)-(24)) and the wall-function method (Eq. (28)). The grids used to obtain the solutions with these methods were 202 × 86 and 120 × 67 respectively, and they both covered a domain with a downstream length of 100 times the inlet height.

The prediction of the reattachment length, x_r, was first investigated. The computed reattachment lengths at Re = 5050 with various models and methods are compared in Table 1, where the Reynolds number, Re, is based on the inlet parameters, i.e. Re = U_0h/ν. The reattachment length was overestimated by Wilcox's k-ω model (WKW) with both the wall-function and the extended-to-wall methods. By contrast, the modified model is able to predict the reattachment length with a much better accuracy.

Table 1. Comparison of the reattachment length, x_r, at Re = 5050.

{}Experiment	SKE*	LSKE †	WKW*	WKW	Present*	Present
6.12W	6.16W	6.10W	6.80W	7.40W	6.12W	6.32W

* computed in conjunction with wall functions.

† computed by Skovgaard and Nielsen [25] with the Launder-Sharma LRN k-ε model.

With the addition of the turbulent cross-diffusion term in the ω-equation, the predicted x_r can be altered by about 10 %. The solution, however, was found to be fairly insensitive to a coefficient c_ω ranged from 0.6 to 1.25. A value of c_ω larger than about 1.8 will make the solution procedure unstable. The coefficient α, by contrast, had a significant effect on the prediction of the reattachment length, x_r, which changes by about 1.4 times the step height with an α variation of 0.1.

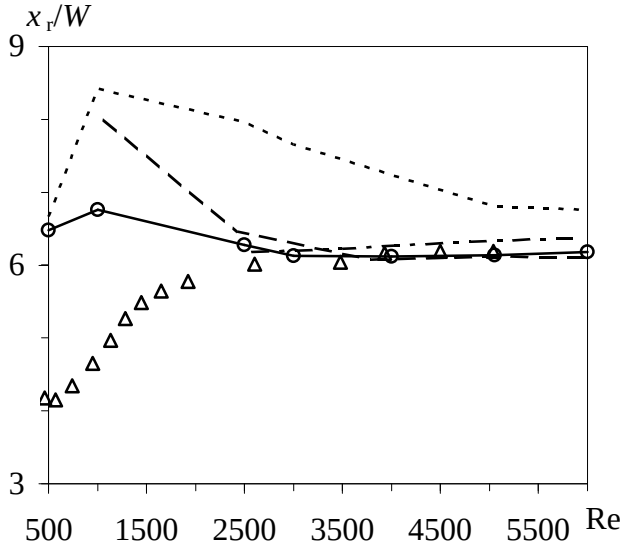

Figure 2. Reattachment length versus Reynolds number, x_r/W ~ Re. – · – · SKE, – – – LSKE, ····· WKW, —○— Present, △ Experimental data [16].

Figure 2 shows the change of the relative reattachment length, x_r/W, with the Reynolds number, Re. The results with the Launder-Sharma LRN k-ε model (LSKE) were computed by Skovgaard and Nielsen [25]. In conjunction with wall functions, the modified k-ω model predicts similar x_r values to those given by the standard k-ε model for Re > 2500. At and below

Re = 2500, the calculations with the k-ω model were all performed with the extended-to-wall method. The inlet boundary condition of ω at such a low Reynolds number cannot be obtained by solving for channel flows with the Lam-Bremhorst LRN k-ε model because the model produces a laminar solution and thus feeds back a zero value to both k and ε. Instead, the solution of the laminar ω-equation for channel flows was used. This solution, together with the laminar parabolic profile of velocity and a very low kinetic energy, e.g. 10^{-10}, were used as the boundary conditions at the inlet for Re ≤ 2500.

As laminar effects become important, there is a range (Re < 1000) where the k-ε model fails to give a converged solution [25]. However, this does not occur when using the k-ω model. The ω-equation, unlike the ε-equation, possesses a solution as the turbulent kinetic energy $k \to 0$ with the convection balanced by the production of ω. Below Re = 1000, therefore, both the original and modified k-ω models are capable of yielding a converged solution. However the predictions differ significantly from the experimental data of Restivo [16]. At Re = 500, the reattachment lengths computed respectively by the modified and original models are very close, because the molecular viscosity now dominates over the eddy viscosity so that both the models tend to return a laminar flow. The models' behavior thus becomes similar.

For the backward-facing step flow at Re = 5050, the distributions of the normalized mean streamwise velocity and the turbulent kinetic energy along different vertical cross-sections are shown in Figures 3 and 4, where U_0 is the air velocity at the inlet. The predictions are compared with Restivo's experimental data [16].

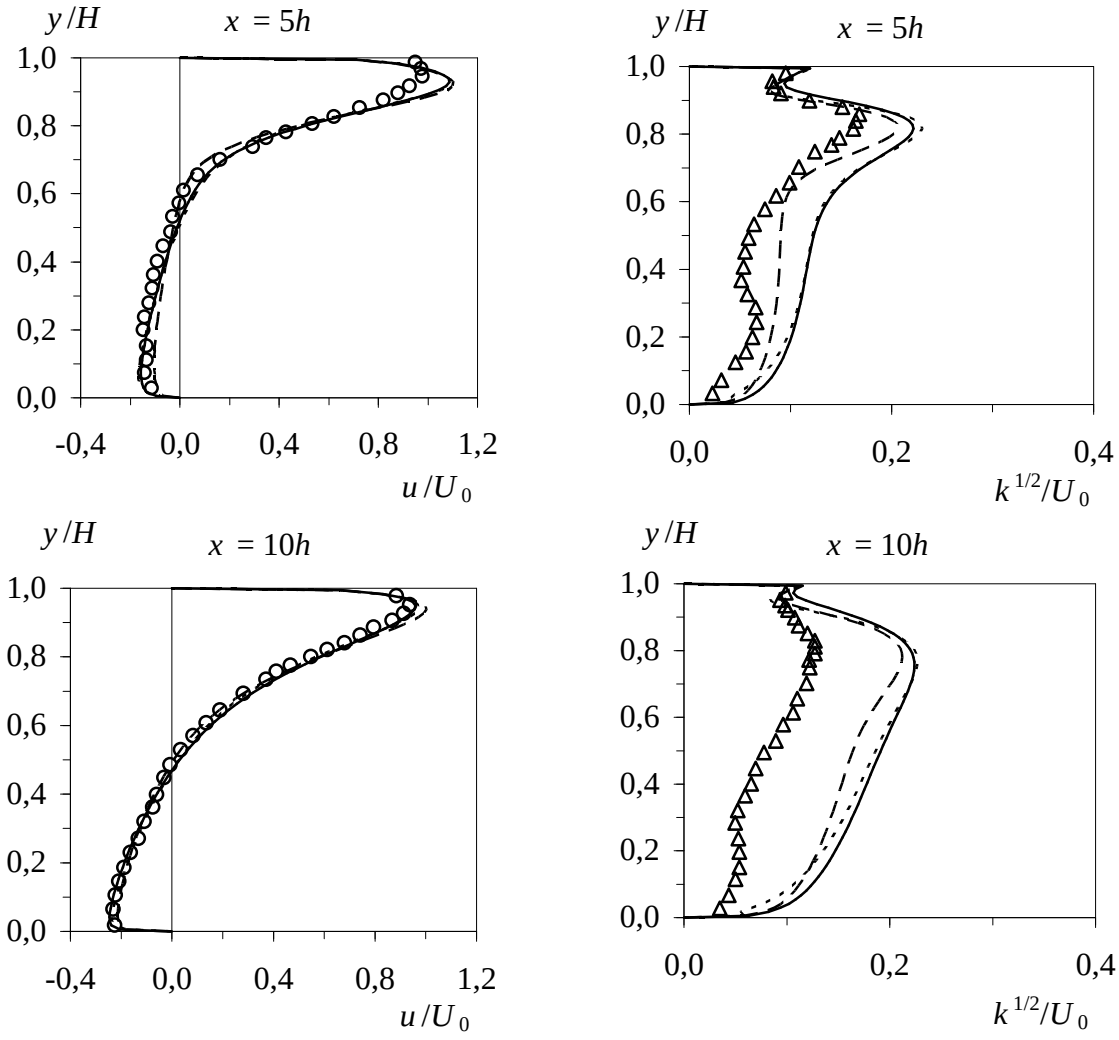

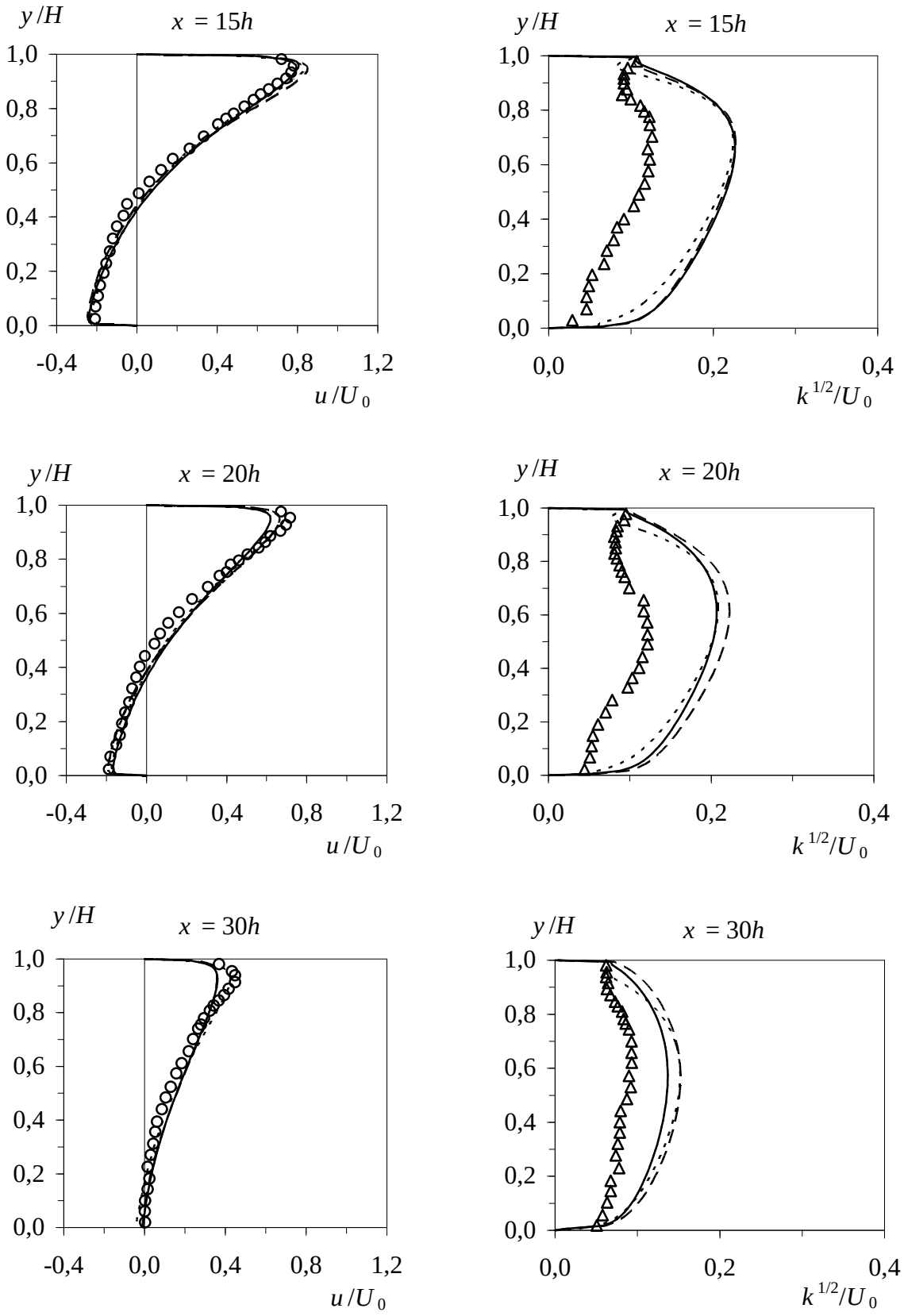

Figure 3. Distributions calculated with the wall-function method. – – – SKE, ····· WKW, —— Present, △ Measured $\sqrt{\overline{u'^2}}$ / U_0 , ○ Measured u/U_0.

Figure 3 shows the results calculated in conjunction with the wall-function method. The variations in the predicted streamwise velocity profiles are very slight, except in the vicinity of the reattachment point. The obvious difference lies mainly in the turbulent kinetic energy, which was overpredicted by all three models. Near the inlet ($x = 5h$), the standard k-ε model produces the closest result to the measured data.

Figure 4 shows the comparison between the modified and the original k-ω models by means of the extended-to-wall method. Using Launder and Sharma's LRN k-ε model, Skovgaard and Nielsen [25] reported a similar prediction. In comparison with the wall-function method, the prediction in Figure 4 is hardly improved even though the grid has been largely refined. Close to both the upper and lower walls, the turbulent kinetic energy predicted by the original model is lower than that by the modified model. Near the upper wall, the underpredicted turbulence level by the original model implies that this model underestimates the near-wall turbulent velocity scale, and thus the eddy viscosity. This explains why the original model overpredicts the reattachment length. The present modification, as expected, enhances the predicted near-wall turbulence energy, particularly after $x = 5h$. The mean streamwise velocity is consequently suppressed in the near-wall region, and the predicted reattachment length thus decreases as desired. The same is also reflected in Figure 3 with the wall-function method.

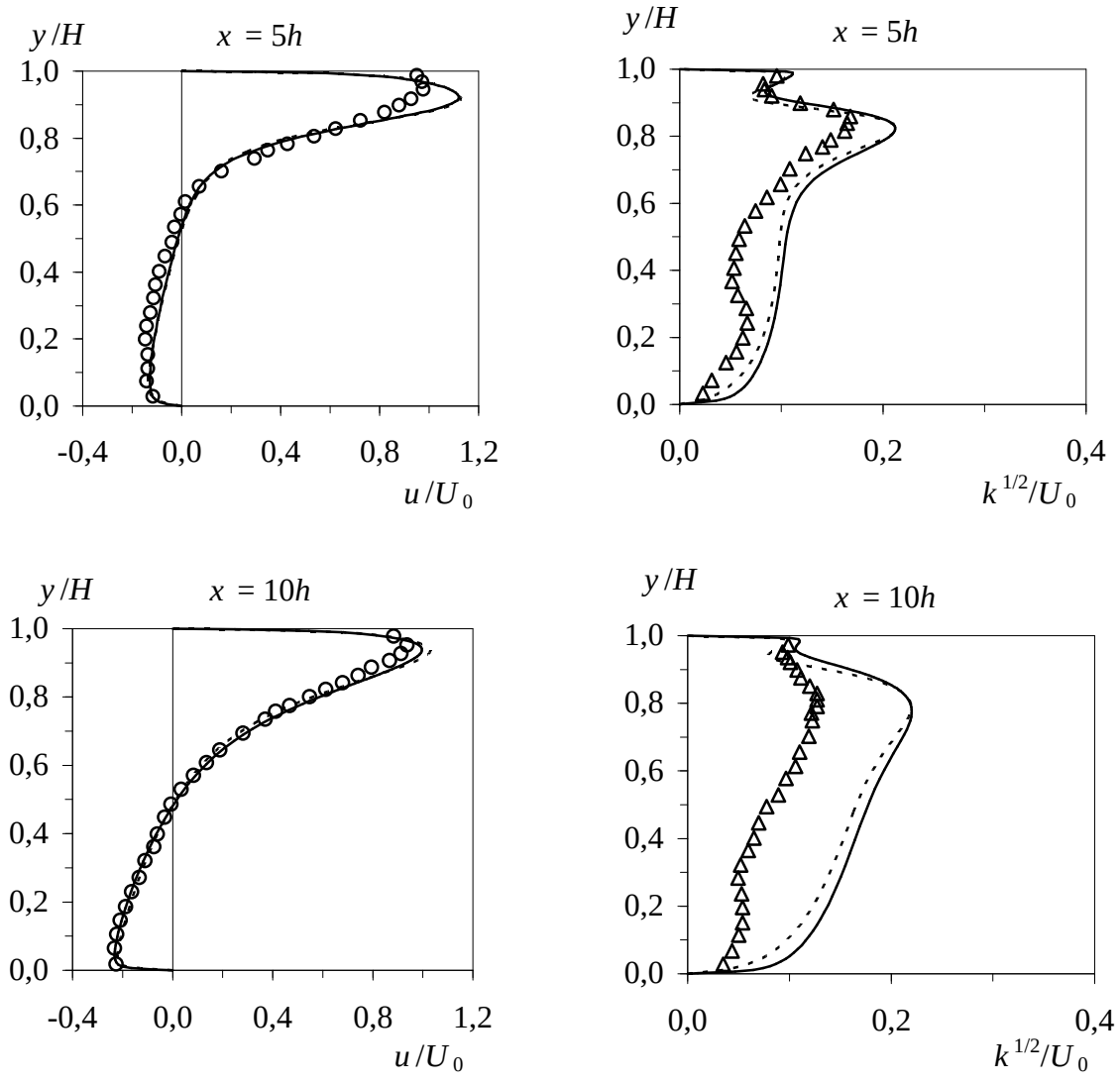

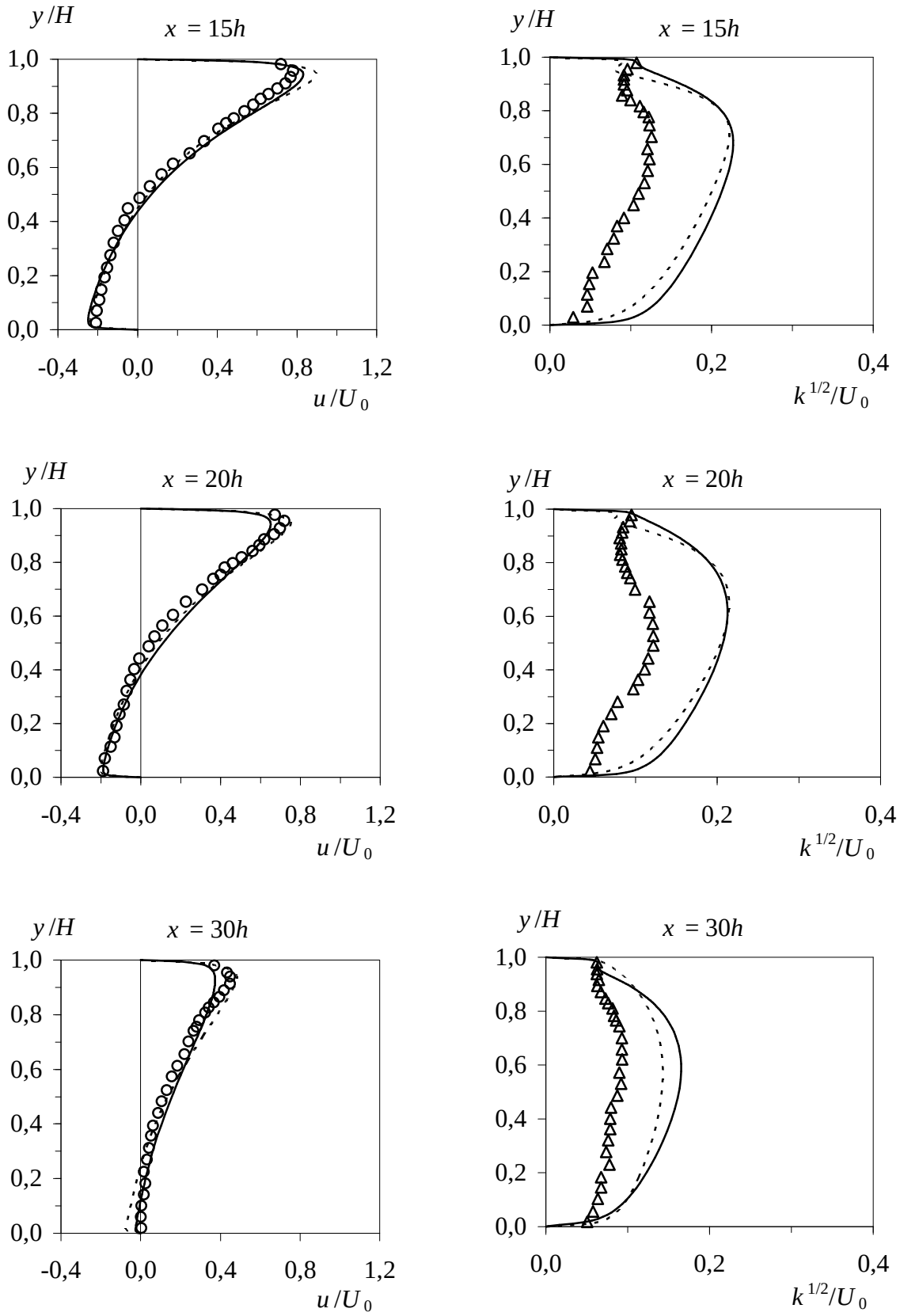

Figure 4. Distributions calculated with the extended-to-wall method. ·····WKW, —— Present, △ Measured $\sqrt{\overline{u'^2}}$ / U_0 , ○ Measured u/U_0.

The results shown above indicate that the modified model is abel to yield satisfactory mean flow profiles, and predict a more accurate reattachment length whether using the wall-function method or using the extended-to-wall method. The near-wall turbulent kinetic energy is enhanced as expected. The predicted tendency of k is similar to that in the experiment. However, all the models considerably overestimate the turbulence level (note that the measured data in the figures are for $\sqrt{\overline{u'^2}}$, and approximately $k^{1/2} \sim 1.1\sqrt{\overline{u'^2}}$ [26]). This inaccuracy is undesirable in ventilation practice because the turbulence level is associated with local drafts.

4.2 Recirculating Flow in a Ventilation Enclosure

The calculations for the backward-facing step flow have shown that an accurate reattachment length can be predicted by the modified k-ω model, which shows a similar performance to the standard k-ε model in conjunction with the wall functions. To further verify this model, the flow in a two-dimensional ventilation enclosure was calculated (Figure 5a), where the inlet-based Reynolds number is 5000. In this flow, a wall-jet initiated from the inlet reaches the opposite wall, and an overall recirculation is created, see Figure 5b. This is a general situation that occurs in a mixing room ventilation. In the following calculations, Lam and Bremhorst's LRN k-ε model (LBKE) was also used for comparison. The calculations were performed with 50×47 cells for the wall-function method, and 102×132 cells for the extended-to-wall method and the LRN k-ε model. The calculated results with various models are compared with Restivo's experimental data [16] (summarized also in [26]) measured along two horizontal cross-sections ($y = h/2$ and $y = H - h/2$) and two vertical cross sections ($x = H$ and $x = 2H$). Note that the measured data used for comparison of the turbulence energy are for $\sqrt{\overline{u'^2}}$, and the calculated results in the following figures have been normalized by parameters based on the inlet velocity and the height of the enclosure, i.e. $U_0 = u_{in}$ and $\omega_0 = u_{in}/H$.

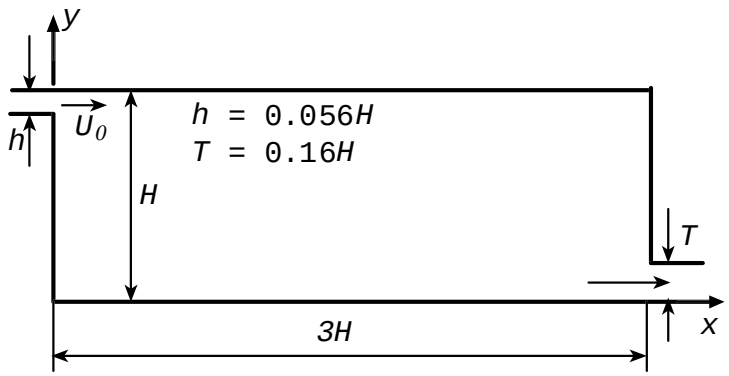

a. Geometry of the ventilation enclosure.

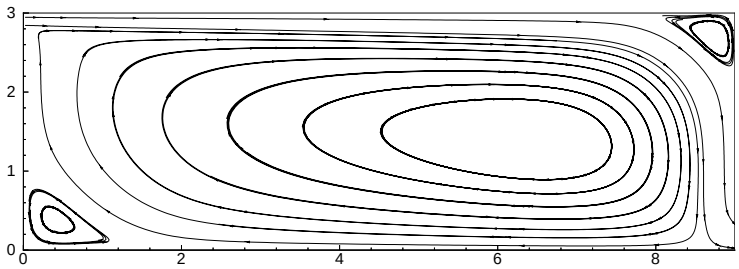

b. Flow field in the ventilation enclosure.

Figure 5. Configuration of the ventilation enclosure.

Figure 6 shows the distributions calculated with the wall-function method. As for the backward-facing step flow, all three models give similar predictions for mean flow profiles. The turbulent kinetic energy is generally well-predicted in the recirculation area as can be seen from the distributions at vertical cross sections $x = H$ and $x = 2H$. In near-wall regions, however, the turbulence level is underestimated by those models. This is also reflected in the distributions along the two horizontal sections, i.e. $y = h/2$ (bottom) and $y = H - h/2$ (top). The original model gives the largest discrepancy in predicting the turbulent kinetic energy. The result, again, suggests that the original model underpredicts the near-wall turbulent velocity scale. The modification does enhance the turbulence level in the near-wall region, but the increment is quite limited. The modified model performs in nearly the same way as the standard k-ε model does. This can also be observed from the distributions of the mean streamwise velocity. In the corner under the inlet (the lower cross-section $y = h/2$), the original model predicts a positive velocity region like in the experiment, but afterwards gives the largest error in the next region. Nevertheless, it means that the secondary eddy in the corner is reproduced by this model. Along the centerline of the inlet (the upper cross-section $y = H - h/2$), the negative velocity near the opposite wall, where a secondary eddy exists, is apparently underpredicted by all the models, and nearly non-negative velocities predicted by the standard k-ε model.

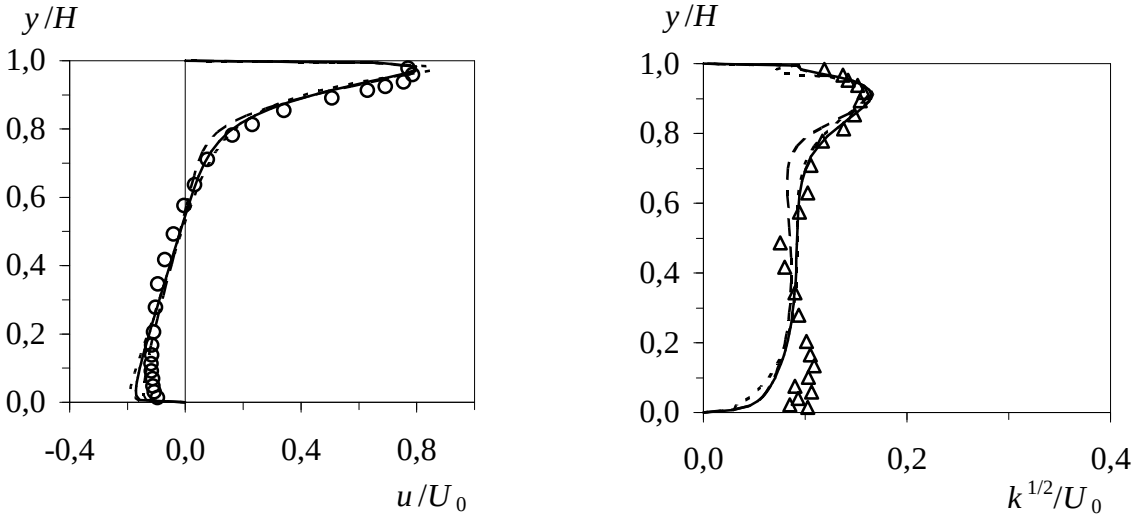

Profiles at vertical cross section $x = H$.

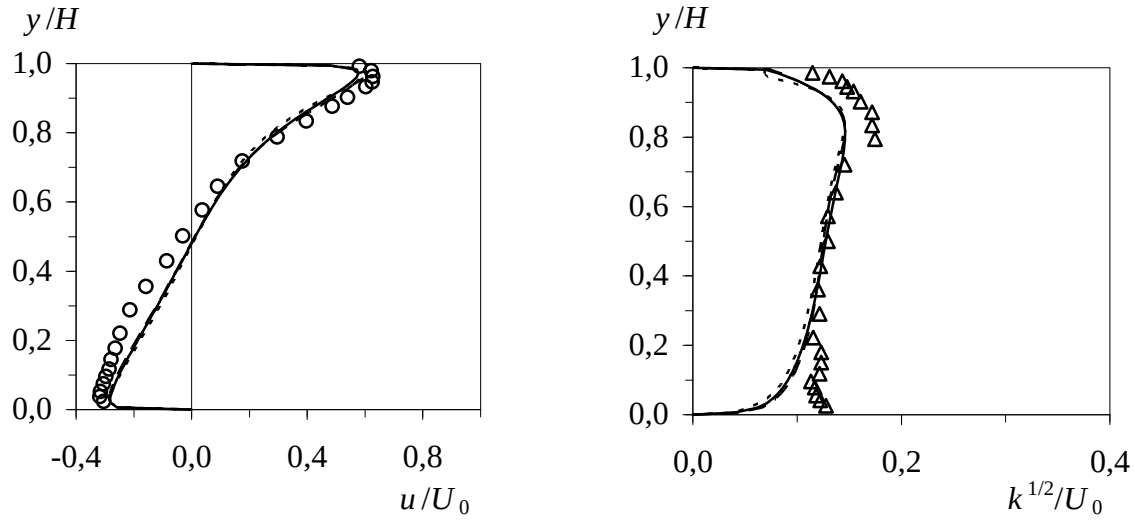

Profiles at vertical cross section $x = 2H$.

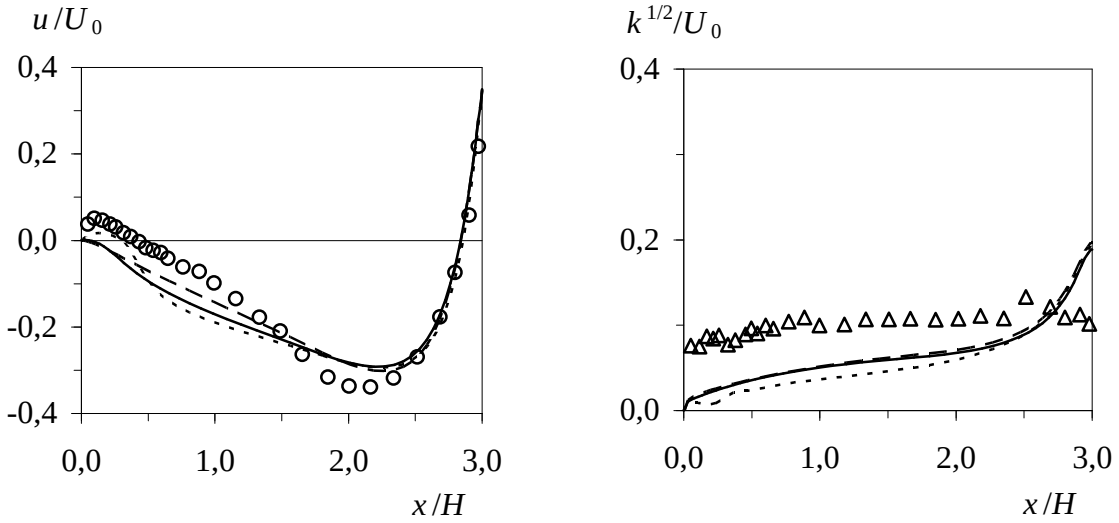

Profiles at horizontal cross section $y = h/2$.

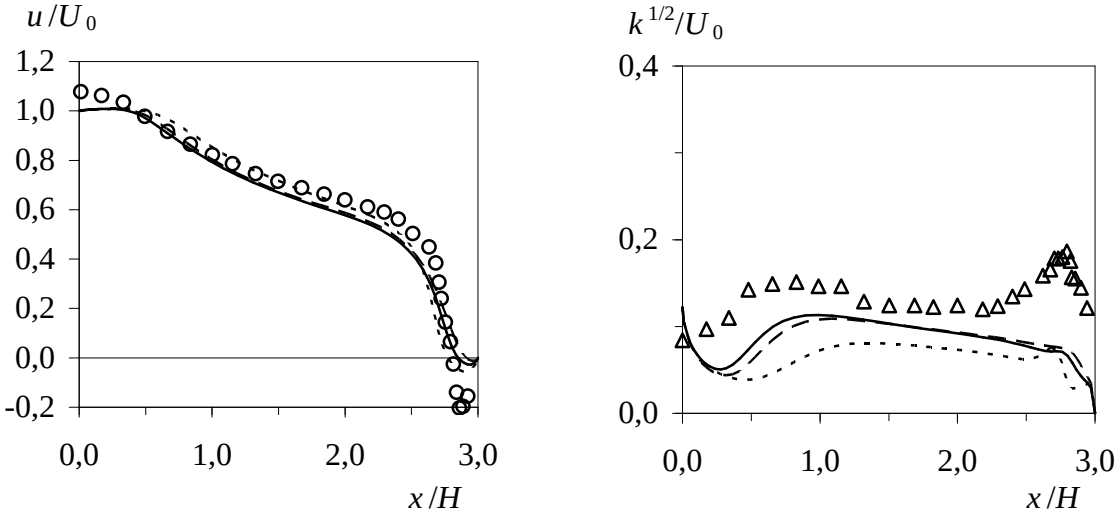

Profiles at horizontal cross section $y = H - h/2$.

Figure 6. Distributions calculated with the wall-function method. – – – SKE, ····· WKW, —— Present, △ Measured $\sqrt{\overline{u'^2}}/U_0$, ○ Measured u/U_0.

With the extended-to-wall method, the predictions are compared in Figure 7. The Lam-Bremhorst LRN k-ε model (LBKE) is now also involved in the comparison. The results shown in Figure 7 are similar to those calculated with the wall-function method in Figure 6. The underestimation by the original model becomes more obvious for the near-wall turbulence level, particularly near the ceiling. The Lam-Bremhorst LRN k-ε mode gives a highest kinetic energy while the original model predicts the lowest. As the wall-jet approaches the opposite wall (see the distributions at the section $y = h/2$), both the original and modified k-ω models reproduce the negative-velocity region though a discrepancy is suffered. The LBKE model, however, does not resolve this secondary bubble in the upper corner near the opposite wall, and thus the negative velocity is hardly predicted. This was also found in [25] which used the Launder-Sharma LRN k-ε model. The result predicted by the modified model is more satisfactory in this region.

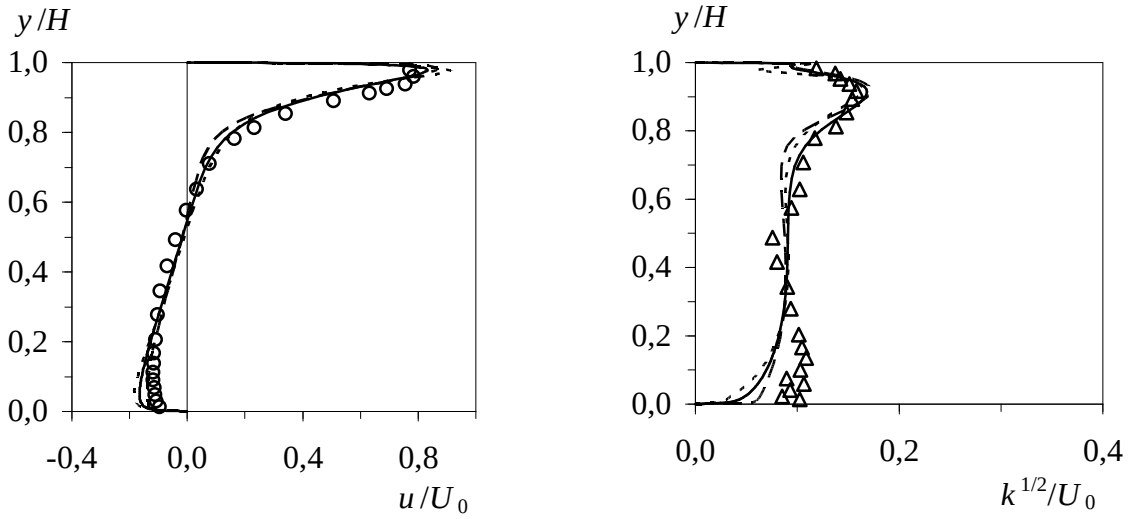

Profiles at vertical cross section $x = H$.

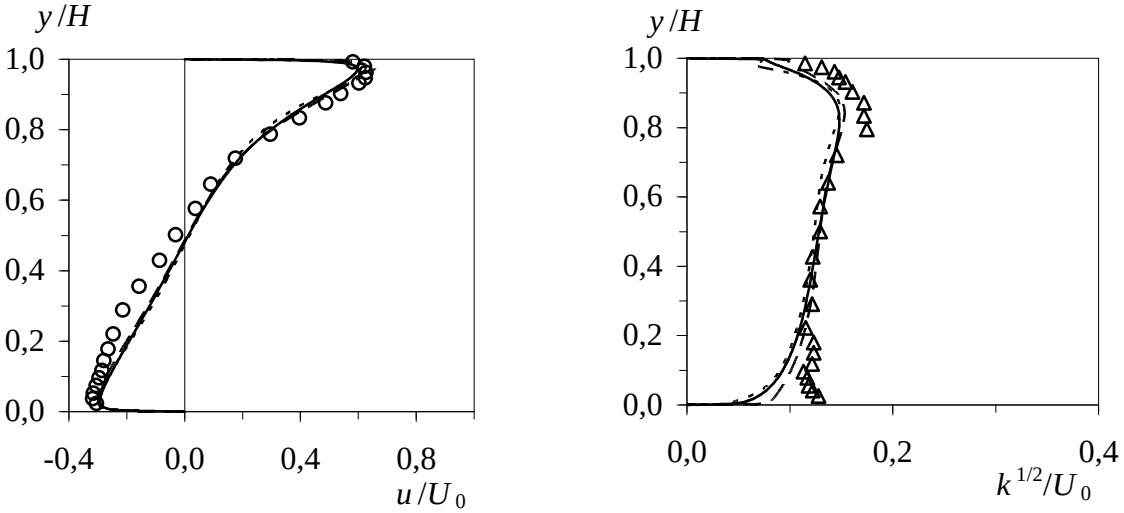

Profiles at vertical cross section $x = 2H$.

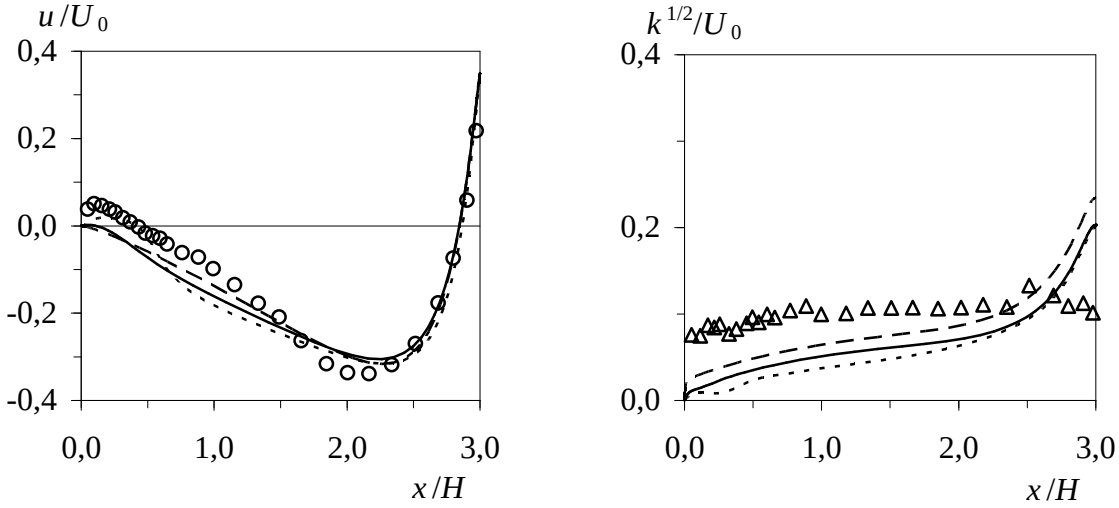

Profiles at horizontal cross section $y = h/2$.

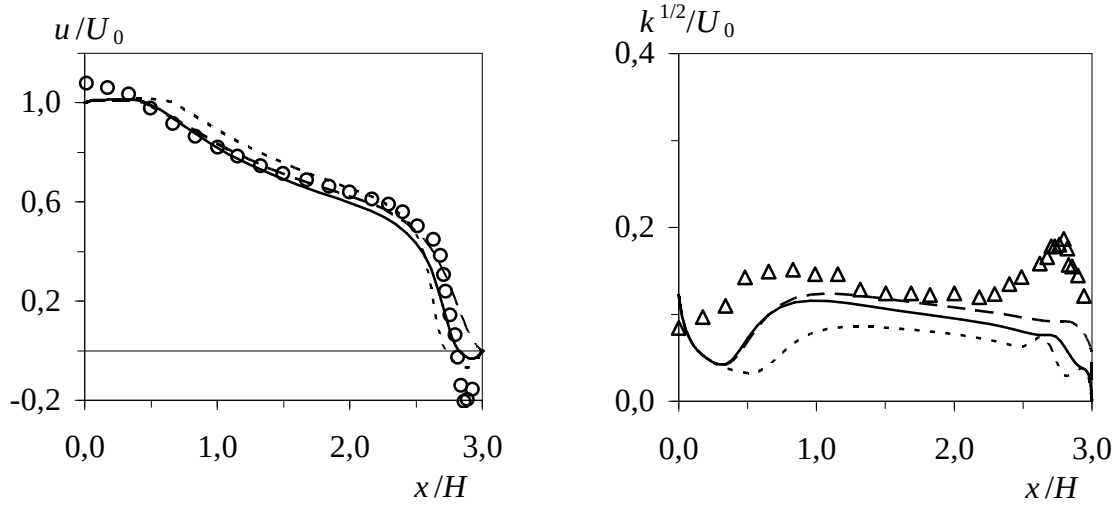

Profiles at horizontal cross section $y = H - h/2$.

Figure 7. Distributions calculated with the extended-to-wall method. – – – LBKE, ····· WKW, —— Present, △ Measured $\sqrt{\overline{u'^2}}\,/\,U_0$, ○ Measured u/U_0.

The distributions of the specific dissipation rate, ω, and the Reynolds shear stress, $-\overline{u'v'}$, are shown in Figure 8. The ω-profile of the LRN k-ε model was calculated from equation (7). In the vertical cross sections, with the modified model, the results are similar to those obtained by the LBKE. The variation can be mainly observed from the horizontal distributions, where the specific dissipation rate of the original model changes quite differently with a peak emerging along the section $y = h/2$. A sharper peak arises also in the section of $y = H - h/2$. The peaks in the distributions of Reynolds shear stress are associated with the positions where the mean velocity changes dramatically. A large change in the velocity may result from a large change in ω or k or both, because they determine the changes in the eddy viscosity that is the only factor the turbulence affects the momentum in the two-equation models. Along the horizontal cross sections, the generally higher ω values computed by the original model are responsible for the lower predictions of the turbulent kinetic energy. All three models give a similar tendency for the Reynolds shear stress, but the confidence of the predictions must be further verified by experiments.

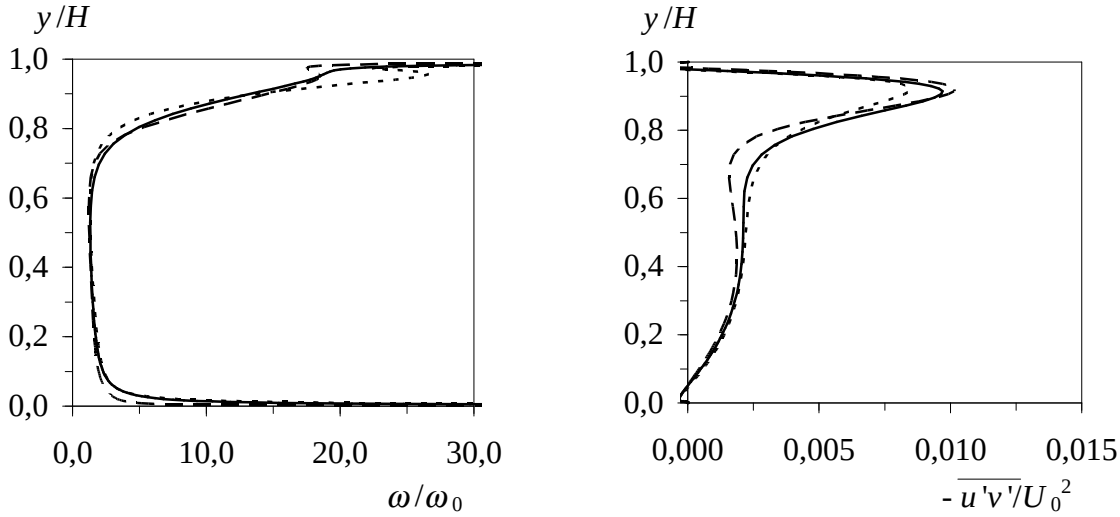

Profiles at vertical cross section $x = H$.

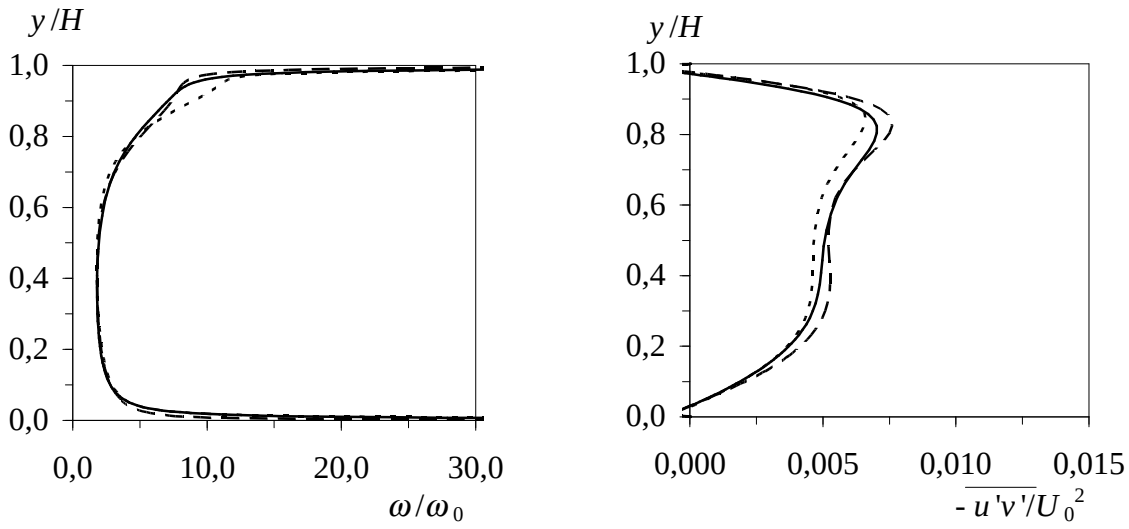

Profiles at vertical cross section $x = 2H$.

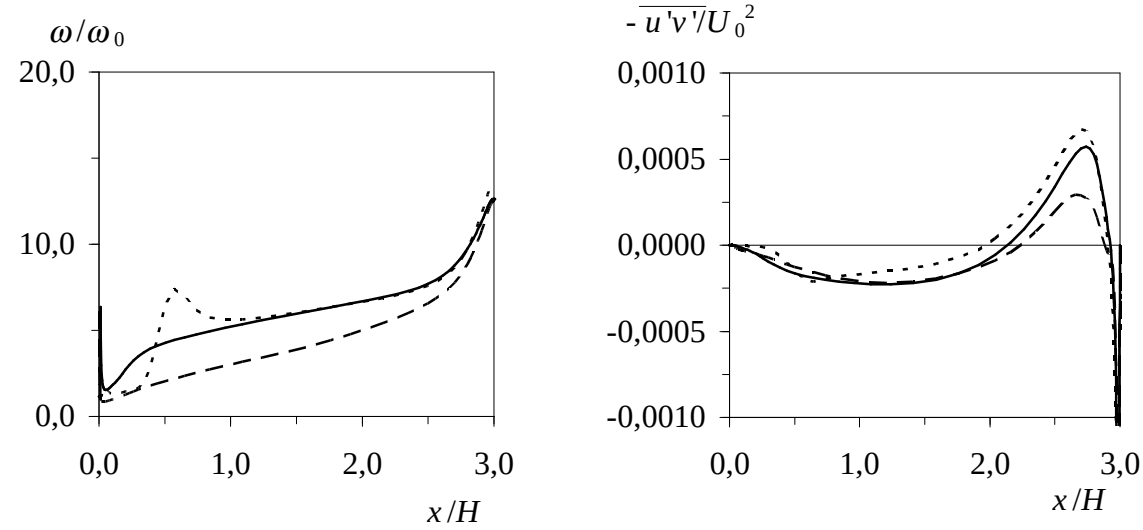

Profiles at horizontal cross section $y = h/2$.

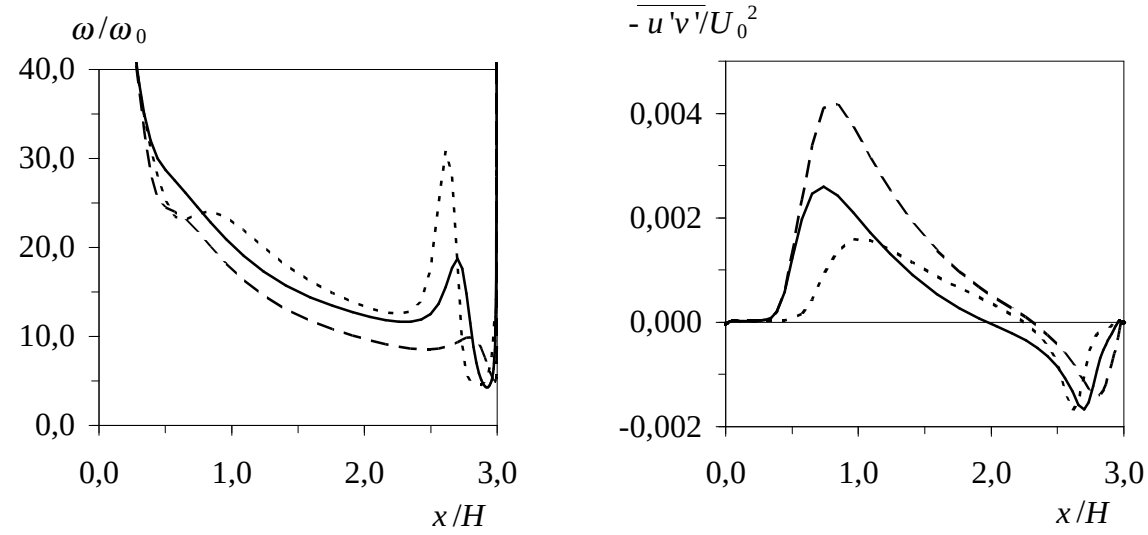

Profiles at horizontal cross section $y = H - h/2$.

Figure 8. Distributions of ω and Reynolds shear stress at various cross sections. – – – LBKE, ····· WKW, —— Present.

The above results show that the modified k-ω model and the k-ε model have a similar performance in the prediction of the recirculating flow in a ventilation enclosure. Although the original model works fairly well for predicting the mean flow profiles, it underestimates the turbulence level with the largest error, particularly in the near-wall regions. In general, this model is slightly weaker than the others whether using the wall-function method or using the extended-to-wall method.

The turbulent cross-diffusion term in the modified ω-equation plays a role mainly in the near-wall region, where the gradients of k and ω are rather large and usually of opposite signs. This will therefore drag down the specific dissipation rate and increase the kinetic energy.

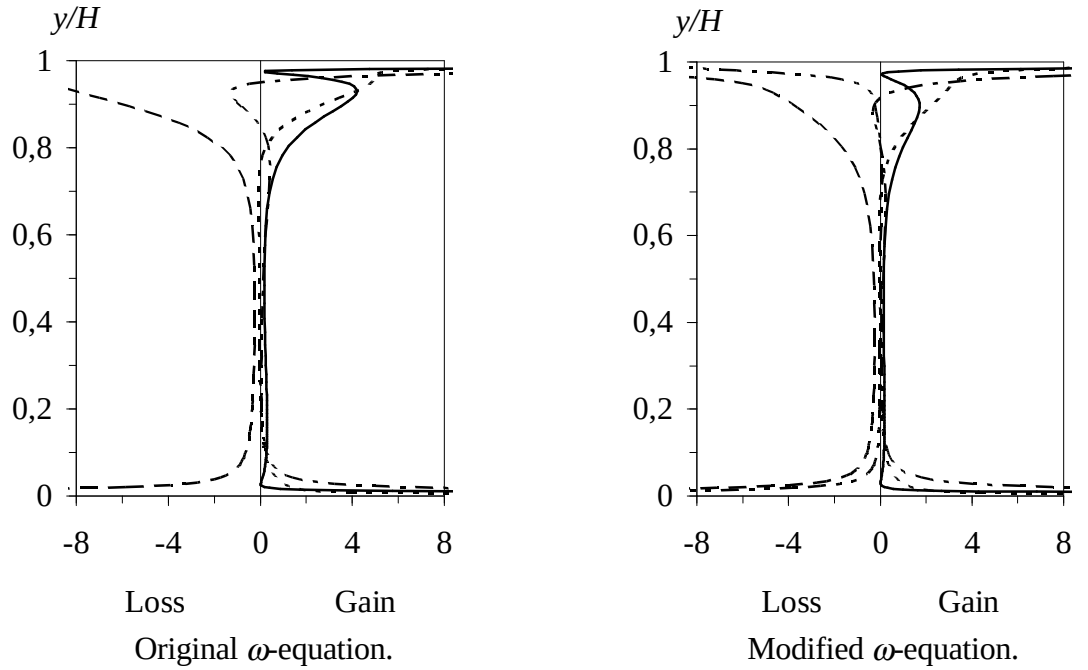

Original ω-equation. Modified ω-equation.

a). Budget at section $x = 2H$.

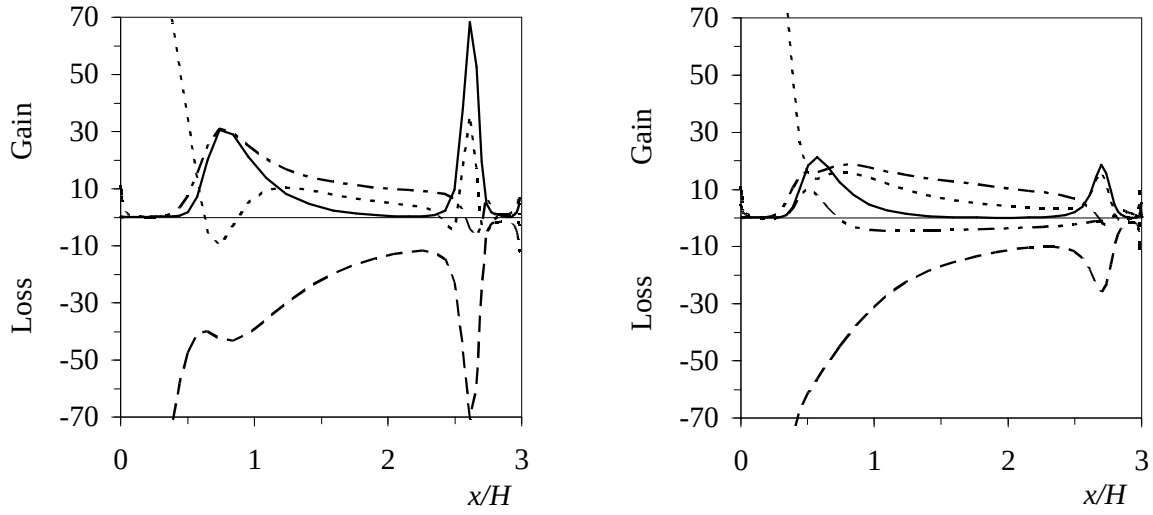

Original ω-equation. Modified ω-equation.

b). Budget at section $y = H\text{-}h/2$.

Figure 9. Budget for the ω-transport equation. ····· Convection, —— Production, – – – Destruction, – · – · Diffusion, – · · – Turbulent cross-diffusion.

Figure 9 shows the budget of the original and modified ω-equations at the sections $x = 2H$ and $y = H - h/2$. The addition of the turbulent cross-diffusion term has redistributed the contribution of each term. Close to the wall, this term in the wall-jet (e.g. at $x = 2H$) is relatively large. The production term, as expected, has been reduced. Along the central line of the wall-jet ($y = H - h/2$), there is a peak in the budgets of both models in front of the opposite wall. This peak is largely damped in the modified ω-equation, owing to the turbulent cross-diffusion term. It explains why the peak in the horizontal ω-distribution at section $y = H - h/2$ is larger with the original model than that with the modified model. This peak corresponds to the turning/separation point in front of the opposite wall, where the wall-jet flow starts to descend.

It should be pointed out that both the original and modified models give an incorrect asymptotic behavior of k with $k \sim y^{3.23}$. With the correct asymptotic behavior for ω and k, i.e. $\omega \sim y^{-2}$ and $k \sim y^2$ as $y \to 0$, the turbulent cross-diffusion term should have a constant limit behavior as the wall is approached. In both the original and modified models, this term will tend to zero as $y \to 0$.

To investigate the numerical performance of the models, Figure 10 shows the maximum normalized residual change with the iteration numbers when calculating the recirculating flow in the confined enclosure. With the Lam-Bremhorst LRN k-ε model, the maximum residual cannot be reduced to 0.001 when starting the calculation with the QUICK scheme. Instead, the results were obtained by using the QUICK scheme re-started with a converged solution obtained by means of the hybrid scheme. The convergence procedure with the LBKE in Figure 10b is thus an illustration of using the hybrid scheme.

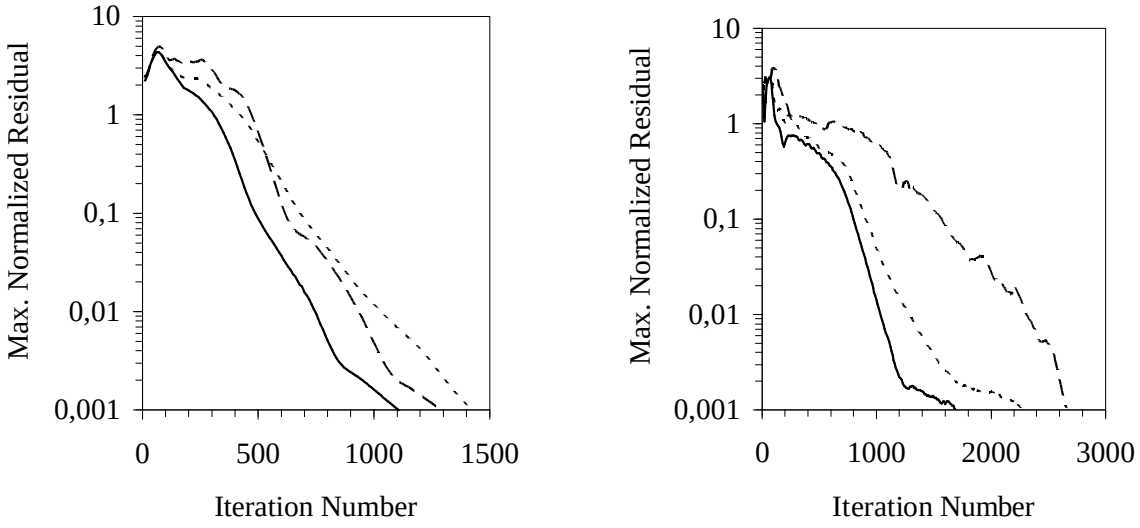

a). Using wall functions. b). Without using wall functions.

Figure 10. Comparison of the convergence procedure with various models. – – – SKE or LBKE, ····· WKW, —— Present.

It is shown that the modified model is more robust in computational efficiency, and the LRN k-ε model has the slowest convergence. One of the reasons for this lies in the fact that the specification of ε at walls has to be coupled with the turbulent kinetic energy during the iteration as shown in equation (25). By contrast, the k-ω models use the asymptotic solution (at the first grid point) as the boundary condition of ω. Moreover, the turbulent cross-diffusion term in the modified ω-equation is usually negative in near-wall regions, which in turn increases the

diagonal dominance of the algebraic equation system and makes the solution procedure more stable when solving the ω-equation. This is reflected in Figure 10 with both the wall-function method and the extended-to-wall method. The modified model achieves a converged solution at the fastest rate. When using the extended-to-wall method, the modified model needs much less iterations than the Lam-Bremhorst LRN k-ε model does. This is certainly preferred in engineering applications since the modified model, on the other hand, possesses a similar numerical performance.

5 Concluding Remarks

The two-equation turbulent k-ω model is implemented to predict recirculating ventilation flows, and the model's performance has been investigated. Both the *extended-to-wall* method and the wall-function method are used in the calculations. The results have been compared with experimental data and predictions by other models.

In comparison with experimental data, Wilcox's original k-ω model overpredicts the reattachment length for the flow over a backward-facing step with an expansion ratio of 5:1. The near-wall eddy viscosity is underestimated by this model. To improve the prediction accuracy, some modifications have been proposed. The model constants are re-evaluated and a turbulent cross-diffusion term is introduced into the ω-transport equation. With these modifications, a far more accurate reattachment length can be predicted when solving for the backward-facing step flow, and the results for the recirculating flow in the two-dimensional ventilation enclosure were also slightly improved, particularly for the prediction of the kinetic energy. The modified model shows a similar performance to the standard k-ε model when using the wall-function method, and to the Lam-Bremhorst LRN k-ε model when using the extended-to-wall method.

The computational effort to achieve a converged solution decreases when using the modified k-ω model. This reduction results from the exact asymptotic boundary condition of ω and the addition of the turbulent cross-diffusion term. This term is usually negative in the near-wall region, and thus able to increase the diagonal dominance of the equation system. The solution procedure consequently becomes more stable. Less computational effort without any loss in computational accuracy is certainly preferred in engineering applications.

The results calculated by the modified model are very encouraging. The present model can be a potential alternative to the conventional k-ε model for simulating air flows in ventilated spaces. In particular, when calculating low-Reynolds-number ventilation flows, the modified k-ω model is worth considering for acceptable predictions of mean flow profiles. Other advantages include the convenience of specifying the wall boundary condition for ω, and not using damping functions as with LRN k-ε models.

References

1 Thangam, S., 1992, "Turbulent Flow Past a Backward-Facing Step: A Critical Evaluation of Two-Equation Models," *AIAA Journal*, Vol. 30, No. 5, pp. 1314-1320.

2 IEA., 1989, "Air Flow Pattern Within Buildings," Flow Flash, No. 1, Int. Energy Agency, *Annex* 20.

3 Chen, Q. and Jiang, Z., 1992, "Significant Questions in Predicting Room Air Motion," *ASHRAE Transaction*, Vol. 98, Part 2, pp. 929-939.

4 Davidson, L., 1989, "Ventilation by Displacement in a Three-Dimensional Room: A Numerical Study," *Building and Environment*, Vol. 24, pp. 263-372.

5 Rotta, J. C., 1968, "Über eine Methode zur Berechnung Turbulenter Scherströmungen," Aerodynamische Versuchanstalt Göttingen, Rep. 69 A14.

6 Zeierman, S. and Wolfshtein, M., 1986, "Turbulent Time Scale for Turbulent-Flow Calculations," *AIAA Journal*, Vol. 24, No. 10, pp. 1606-1610.

7 Speziale, C. G., Abid, R. and Anderson, E. C., 1992, "Critical Evaluation of Two-Equation Models for Near-Wall Turbulence," *AIAA Journal*, Vol. 30 No. 2, pp. 324- 325.
8 Saffman, P. G., 1970, "A Model for Inhomogeneous Turbulent Flow," *Proc. Roy. Soc*., London, Vol. A317, pp. 417-433.
9 Wilcox, D. C. and Rubesin, M. W., 1980, "Progress in Turbulence Modelling for Complex Flow Fields Including Effects of Compressibility," *NASA TP* 1517.
10 Ilegbusi, J. O. and Spalding, D. B., 1985, "An Improved Version of the *k-w* Model of Turbulence," ASME *Journal of Heat transfer*, Vol. 107, No. 2, pp. 63-69.
11 Wilcox, D. C., 1988, "Reassessment of the Scale-Determining Equation for Advanced Turbulence Models," *AIAA Journal*, Vol. 26, No. 11, pp. 1299-1310.
12 Wilcox, D. C., 1994, "Simulation of Transition with a Two-Equation Turbulence Model," *AIAA Journal*, Vol. 32, No. 2, pp. 247-254.
13 Menter, F. R., 1994, "Two-Equation Eddy-Viscosity Turbulence Models for Engineering Applications," *AIAA Journal*, Vol. 32, No. 8, pp. 1598-1604.
14 Liu, F. and Zheng, X., 1994, "Staggered Finite Volume Scheme for Solving Cascade Flow with a k-ω Turbulence Model," *AIAA Journal*, Vol. 32. No. 8, pp. 1589-1596.
15 Patel, V. C. and Yoon, J. Y., 1995, "Application of Turbulence Models to Separated Flow over Rough Surfaces," ASME *Journal of Fluid Engineering*, Vol. 117, No. 6, pp. 234-241.
16 Restivo, A. M. O., 1979, "Turbulent Flow in Ventilated Rooms," Ph. D. Thesis, Imperial College, Mech. Eng. Department, London.
17 Peng, S., 1995, Unpublished Calculations, Dept. of Thermo and Fluid Dynamics, Chalmers Univ. of Tech., Gothenburg.
18 Lumley, J. L., 1978, "Computational Modeling of Turbulent Flow," *Adv. Appl. Mech.*, Vol. 18, pp. 124-176.
19 Davidson, L. and Farhanieh, B., 1991, "CALC-BFC: A Finite-Volume Code Employing Collocated Variable Arrangement and Cartesian Velocity Components for Computation of Fluid Flow and Heat Transfer in Complex Three-Dimensional Geometries," Dept. of Thermo and Fluid Dynamics, Chalmers Univ. of Tech. Gothenburg.
20 Patankar, S. V., 1981, "Numerical Heat Transfer and Fluid Flow," McGraw-Hi, Washington.
21 Rhie, C. M. and W. L. Chow, 1983, "Numerical Study of the Turbulent Flow Past an Airfoil with Trailing Edge Separation," *AIAA Journal*, Vol. 21, No. 11, pp. 1525-1532.
22 Leonard, B. P., 1979, "A Stable and Accurate Convective Modeling Procedure Based on Quadratic Upstream Interpolation," *Computer Methods in Appl. Mech. and Eng.*, Vol. 19, pp. 59-98.
23 Stone, H. L., 1968, "Iterative Solution of Implicit Approximations of Multidimensional Partial Differential Equations," *SIAM J. Num. Anal.*, Vol. 5, pp. 530-558.
24 Lam, C. K. G. and Bremhorst, K. A., 1981, "Modified Form of the k-ε Model for Predicting Wall Turbulence," ASME *Journal of Fluids Engineering*, Vol. 103, pp. 456-460.
25 Skovgaard, M., 1991, "Turbulent Flow in Rooms Ventilated by Mixing Principle," Ph. D. Thesis, Dept. of Building Tech. and Structural Eng., Aalborg Univ., Aalborg.
26 Nielsen, P. V., 1990, "Specification of a Two-Dimensional Test Case," Dept. of Building Tech. and Structural Eng., Aalborg Univ., Aalborg.

Filename: PAPER01.DOC
Directory: C:\PENG\ARTICLES\RP_NIW~1
Template: C:\PROGRAM\OFFICE\WINWORD\TEMPLATE\NORMAL.DOT
Title: The Two-Equation Turbulence k-w Model Applied to Recirculating Ventilation Flows
Subject:
Author: Shia-hui Peng
Keywords:
Comments:
Creation Date: 98-09-01 09:31
Revision Number: 113
Last Saved On: 98-09-03 13:07
Last Saved By: Shia-hui Peng
Total Editing Time: 458 Minutes
Last Printed On: 98-09-03 16:29
As of Last Complete Printing
Number of Pages: 25
Number of Words: 6 861 (approx.)
Number of Characters: 39 111 (approx.)